RESEARCH ARTICLE

Enduring alterations in hippocampal astrocyte-synaptic proximity following adolescent alcohol exposure: reversal by gabapentin

Kati L. Healey[1], Sandra Kibble[1], Sierra Hodges[1], Kathryn J. Reissner[2], Anze Testen[2], Tiffany A. Wills[3], Shawn K. Acheson[1], Benjamin M. Siemsen[4], John A. McFaddin[4], Michael D. Scofield[4,#], H. Scott Swartzwelder[1,*,#]

1 Department of Psychiatry and Behavioral Sciences, Duke University Medical Center, Durham, NC, USA
2 Department of Psychology and Neuroscience, University of North Carolina, Chapel Hill, NC, USA
3 Department of Cell Biology and Anatomy, LSU School of Medicine, New Orleans, LA, USA
4 Department of Anesthesia and Perioperative Medicine, Medical University of South Carolina, Charleston, SC, USA

Funding: *This study was supported by the National Institute on Alcohol Abuse and Alcoholism (NIAAA) Neurobiology of Adolescent Drinking In Adulthood (NADIA) Grant # 2U01AA019925 (to HSS); the National Institute on Alcohol Abuse and Alcoholism (NIAAA) R00AA022651 (to TAW); the National Institute on Drug Abuse (NIDA) R01DA041455 (to KJR).*

Abstract

Adolescent alcohol abuse is a substantive public health problem that has been the subject of intensive study in recent years. Despite reports of a wide range of effects of adolescent intermittent ethanol (AIE) exposure on brain and behavior, little is known about the mechanisms that may underlie those effects, and even less about treatments that might reverse them. Recent studies from our laboratory have indicated that AIE produced enduring changes in astrocyte function and synaptic activity in the hippocampal formation, suggesting the possibility of an alteration in astrocyte-neuronal connectivity and function. We utilized astrocyte-specific, membrane restricted viral labeling paired with immunohistochemistry to perform confocal single cell astrocyte imaging, three-dimensional reconstruction, and quantification of astrocyte morphology in hippocampal area CA1 from adult rats after AIE. Additionally, we assessed the colocalization of astrocyte plasma membrane labeling with immunoreactivity for AMPA-(α-amino-3-hydroxy-5-methyl-4-isoxazolepropionic acid) glutamate receptor 1, an AMPA receptor subunit and established neuronal marker of excitatory synapses, as a metric of astrocyte-synapse proximity. AIE significantly reduced the colocalization of the astrocyte plasma membrane with synaptic marker puncta in adulthood. This is striking in that it suggests not only an alteration of the physical association of astrocytes with synapses by AIE, but one that lasts into adulthood - well after the termination of alcohol exposure. Perhaps even more notable, the AIE-induced reduction of astrocyte-synapse interaction was reversed by sub-chronic treatment with the clinically used agent, gabapentin (Neurontin), in adulthood. This suggests that a medication in common clinical use may have the potential to reverse some of the enduring effects of adolescent alcohol exposure on brain function. All animal experiments conducted were approved by the Duke University Institutional Animal Care and Use Committee (Protocol Registry Number A159-18-07) on July 27, 2018.

****Correspondence to:***
H. Scott Swartzwelder, PhD, hss@duke.edu.

#Both authors contributed equally to this work.

orcid:
0000-0001-5845-1670 (H. Scott Swartzwelder)

doi: *10.4103/1673-5374.274339*

Received: *September 25, 2019*
Peer review started: *September 29, 2019*
Accepted: *October 7, 2019*
Published online: *January 28, 2020*

Key Words: *adolescent; alcohol; astrocyte; astrocyte morphology; astrocyte-neuronal colocalization; CA1; gabapentin; GluA1; hippocampus; tripartite synapse*

Chinese Library Classification No. *R453; R364; R749*

Introduction

Adolescence is a critical period for the development and maturation of neural circuitry, a process that is required for the emergence of cognitive processes necessary for successful adult function. The initiation of drinking during adolescence is associated with a four-to-five-fold greater risk of developing alcohol abuse disorders in adulthood (Dawson et al., 2008), and with cognitive deficits, particularly in the domains of memory and mood disorders (Spear, 2018). Binge pattern alcohol exposure during adolescence alters brain morphology and function in both humans and animal models, and those brain changes may be a driving force underlying the cognitive and affective deficits seen after chronic alcohol use in adolescence.

The hippocampal formation is critical for both cognitive and affective functioning, and has been shown to be powerfully affected, both histologically (Mulholland et al., 2018), and physiologically (Swartzwelder et al., 2017) by adolescent intermittent ethanol (AIE) exposure [see Crews et al. (2019) for review]. One plausible mechanism underlying the synaptic and morphological changes observed in the hippocampus after AIE is an alteration of astrocyte function and a disruption of the physical interaction between astrocytes and neurons. Astrocytes modulate neuroinflammation, synaptic plasticity, neurotransmission (Volterra and Meldolesi, 2005), synaptogenesis and physically interact with neurons (Eroglu, 2009). In addition, it has recently become clear that AIE produces persistent alterations in astrocyte activation and release of thrombospondins (TSPs), which regulate synaptogenesis and function, as well as levels of the neuronal α2δ1 receptor to which TSPs bind (Risher et al., 2015a). Interestingly, these changes persist into adulthood long after the end of the alcohol exposure (Risher et al., 2015a). This suggests that AIE induces an enduring change in astrocyte function

that may be linked to the mechanistic underpinnings responsible for long lasting hippocampal, cognitive, and affective effects of adolescent alcohol exposure.

Despite recent advances, it remains unclear whether AIE induces a long-lasting change in astrocyte-neuronal coupling. Therefore, we designed the present experiment to assess the effect of AIE on the proximity of astrocytic processes to synapses in area CA1 of the hippocampus of adult rats. We hypothesized that AIE would diminish astrocytic ensheathment of synapses and that gabapentin would reverse or attenuate this AIE-induced decrease in astrocyte-synaptic contacts.

Materials and Methods

Animals, ethanol exposure, and gabapentin injections

The following techniques used in this experiment were conducted in accordance with the guidelines of the American Association for the Accreditation of Laboratory Animal Care and the National Research Council's Guide for Care and Use of Laboratory Animals and were approved by the Duke University Institutional Animal Care and Use Committee (Protocol Registry Number A159-18-07) on July 27, 2018.

Experiment 1: Astrocyte-synapse colocalization assay

Thirty-five adolescent male Sprague-Dawley rats (Charles River, Raleigh, NC, USA; postnatal day (PND) 25; ~100 g) were given 5 days to adjust to the vivarium on a reversed 12-hour light: 12-hour dark cycle. Animals were double housed upon arrival with ad libitum access to food and water. Beginning on PND30, intermittent dosing with ethanol (Decon Labs, Prussia, PA, USA) (5 g/kg, i.g., 35% EtOH) or isovolumetric water (AIW) was administered during adolescence (PND31–46) as previously described (Swartzwelder et al., 2019). Briefly, animals were dosed on a 2-day on, 1-day off, 2-day on, 2-day off schedule for a total of 16 doses. This ethanol dose was selected to cause blood ethanol concentrations that are consistent with those achieved by human adolescents during binge drinking episodes (Lees et al., 2019). To minimize stress to experimental animals we routinely assess blood ethanol concentrations in sentinel animals rather than expose experimental animals to the stress of blood sampling. We have found that rats of the age, sex, and strain used in this study that receive 5 g/kg ethanol (i.g.) achieve mean blood ethanol concentrations of 199.7 ± 19.9 mg/dL 60 minutes after the first AIE dose, and 172.8 ± 13.3 mg/dL 60 minutes after the last AIE dose (Risher et al., 2015a). Blood ethanol concentrations in that range are observed consistently in our studies (Risher et al., 2013). One-week following the last ethanol or water dose, surgeries were performed (see below). Approximately 2 weeks after virus surgery (described below), gabapentin (100 mg/kg in sterile 0.9% NaCl, i.p.; Chem-Impex International, Inc., Wood Dale, IL, USA) or isovolumetric saline injections were initiated. Animals were treated daily for 5 consecutive days. Forty-eight hours after the last dose, all animals were sacrificed via cardiac perfusion and brain tissue harvested.

Viral surgery

One week after the last ethanol or water dose, all animals underwent stereotaxic surgery for viral injection into the right hippocampus (–3.2 A/P; 2.6 M/L; –3.2 D/V; Paxinos and Watson, 1986). Briefly, 1μL of rAAV5/GFAP-LCK-GFP(LCK-GFP), obtained from the UNC vector core at ~1 × 10^{12} viral particles/mL, was infused using a 33-gauge injector needle, at a rate of 0.1 μL/min followed by 15 minutes of diffusion time (Scofield et al., 2016; Testen et al., 2018; Siemsen et al., 2019a).

Immunohistochemistry

Forty-eight hours after the last gabapentin injection, animals were sacrificed by cardiac perfusion under isoflurane anesthesia (4% paraformaldehyde, two-hour post-fix then transferred to 30% sucrose PBS solution). 100-μm coronal slices were taken on a Leica vibratome, sections containing the hippocampus were blocked with 2% NGS and 2% Triton-X 100 in 0.1 M PBS (PBST) for 1.5 hours. Sections were then incubated in primary antibodies (Chicken anti-GFP, Abcam, Cambridge, MA, USA, 1:1000, Cat# Ab13970; anti-AMPA receptor 1, Cell Signaling Technology, Danvers, MA, USA, 1:500, Cat# 13185) diluted in PBST with shaking overnight at 4°C. Sections were washed three times, for 5 minutes each, in PBST before secondary incubation was performed at room temperature for 5 hours, with species-appropriate secondary antibodies (goat anti-chicken, Alexa-Flour 488, Cat# ab150169; 1:2000, Life Technologies, Carlsbad, CA, USA) in PBST. Slices were washed after secondary antibody incubation three times, for five minutes each, in PBST prior to mounting with Pro Long Gold Antifade (Life Technologies). The immunohistochemistry procedures utilized were optimized by the Scofield laboratory and ours (Scofield et al., 2016; Testen et al., 2019).

Imaging

Astrocyte image acquisition and the subsequent colocalization assay were performed as described previously (Scofield et al., 2016; Siemsen et al., 2019a; Testen et al., 2019). Briefly, astrocytes with clear boundaries were imaged, provided that no obvious interruptions of the LCK-GFP signal were observed. Averages of five hippocampal astrocytes per animal were acquired, along with synaptic puncta, by an investigator blind to treatment groups. Acquisition of images was performed on a Leica SP8, laser scanning, confocal super-resolution microscope equipped with HyD detectors and a 63× objective (NA 1.4; Leica, Buffalo Grove, IL, USA). Images were acquired at 2048 × 2048, with a pinhole of 1 Airy unit, and a z-step size of 0.3 μm. These settings produce data sets with X, Y and Z dimensions of 60 nm × 60 nm × 300 nm. Confocal data sets were deconvolved using Huygens Hyvolution software (Scientific Volume Imaging, VB Hilversum, Netherlands), embedded within the Leica image acquisition software. Following deconvolution, data sets were imported into Imaris for digital rendering (Bitplane, Zurich, Switzerland). A blinded experimenter isolated the boundary of individual astrocytes using the surface function to generate a region of interest (ROI). Both volume and surface area were calculated from this isolated ROI. Morphological data were expressed as surface area/volume as described previously (Siemsen et al., 2019b).

Proximity of astrocyte processes to synapses was estimated by measuring colocalization of the virally labeled astrocyte plasma membrane signal with the punctate synaptic marker (GluA1). For detailed methods see (Siemsen et al., 2019a). We chose GluA1 as a marker of synaptic puncta because of its abundance at the post-synaptic density and because of

the high quality of anti-GluA1 antibodies. For example, we have used GluA1 and demonstrated its enrichment in large dendritic spines (Siemsen et al., 2019b). To avoid bias, signal intensity thresholds for colocalization were automatically determined using the Costes estimation function (Costes et al., 2004), embedded within the colocalization module of the Imaris software. The volume (μm^3) of 'colocalized' voxels was normalized from cell to cell by expressing the volume of colocalized signal relative to the volume (μm^3) of the corresponding astrocyte, yielding single-cell values for astrocyte-synaptic proximity, reported here as %ROI colocalization. As a control, the number of synaptic puncta was also determined using Imaris, via the spots function, by virtue of intensity for the GluA1 signal. In this analysis, signal intensity thresholds were also determined automatically with Imaris. To analyze synapse density, GluA1 puncta number values were normalized to the overall voxel count in the deconvolved z-series (yielding synaptic puncta per voxel or synapse density).

Experiment 2: GluA1 protein expression

Twelve adolescent male Sprague-Dawley rats (Charles River; PND25; ~100 g) were randomly and equally divided into AIW or AIE treatment groups and dosed as described in Experiment 1.

Tissue preparation

In adulthood (PND70-75), rats were deeply anesthetized with a bell-jar administered isoflurane inhalation [30% v/v at ~1.0 mL of isoflurane per 500 mL volume of jar; Henry Schein Animal Health, Portland, ME, USA (provided by Duke Division of Laboratory Animal Resources Pharmacy)], rapidly decapitated, and brains were harvested for hippocampal GluA1 analyses. CA1 tissue punches were dissected and rinsed very briefly in cooled PBS. For CA1 tissue punch preparation, the whole brain was placed in a chilled stainless-steel brain matrix (Stoelting, Wood Dale, IL, USA). Surgical carbon steel blades were used to obtain 1mm coronal slices and CA1 hippocampus was dissected out using a 1mm micro-punch (Ted Pella Inc., Redding, CA, USA). The tissue was collected, quick frozen and shipped overnight to Vanderbilt University for Western blot analysis. Tissue was prepared in homogenization buffer (150 mM KCl, 50 mM Tris-HCl pH 7.5, mM dithiothreitol (DTT), 0.2 mM phenylmethylsulfonyl fluoride (PMSF), 1 mM benzamidine, 1 µM pepstatin, 10 µg/mL leupeptin, and 1 µM microcystin-leucine, arginine (MC-LR) using Teflon-glass tissue grinder (Wheaton, Millville, NJ, USA) with a motorized plunger at 4°C (Gustin et al., 2011; Baucum et al., 2013).

Immunoblot analysis

The protein concentration of homogenized samples was determined using a Thermo Scientific™ NanoDrop™ 2000 (Spectrophotometers, Waltham, MA, USA) and samples were adjusted to achieve equal protein concentration. The proteins were resolved by sodium dodecyl sulfate-polyacrylamide gel electrophoresis (SDS-PAGE) and transferred to nitrocellulose membranes. Nitrocellulose membranes were blocked in 5% milk in tris-buffered saline with 0.1% tween-20 (TBST) and incubated overnight at 4°C with the GluA1 antibody (Santa Cruz Biotechnology, Santa Cruz, CA, USA, Cat# sc-13152, RRID:AB_627932; 1:1000). For detection using the Odyssey system (LiCor Biosciences, Lincoln, NE, USA), infrared-conjugated secondary antibody (Mouse-800 & Rabbit-700 incubated for 1 hour at room temperature; LiCor; 1:10,000) were used. Densitometry was performed using Image J (National Institutes of Health, Bethesda, MD, USA) on images linearly adjusted for brightness and contrast. Inputs were normalized to Ponceau-S staining as a loading control.

Statistical analyses

All analyses were performed using SPSS (v25.0) (IBM, Armonk, NY, USA). The terminal point of observation involved individual cells nested within animals. To maximize statistical power without inflating Type I error, multilevel modeling was implemented using the SPSS Mixed Linear Modeling procedure (Aarts et al., 2014; Testen et al., 2018, 2019). Animal number was used as the nested variable. AIE and gabapentin were treated as fixed effect independent variables. Dependent variables included %ROI colocalization, GluA1 puncta density, and the ratio of astrocyte surface area to volume. Our specific hypotheses were assessed using simple main effects analyses. Alpha was set at $P < 0.05$ for all simple main effects analyses, and at $P < 0.1$ for the AIE by gabapentin interaction, for purposes of analyzing simple main effects, because of the low power of interactions at a given sample size relative to main effects (Snedecor and Cochran). One-tailed alpha criteria were used for simple main effects given the directional specificity of our hypotheses. The estimated marginal means accounting for the covariance attributed to nested effects are reported in **Figures 1** and **2**.

Results

Astrocyte morphology

The viral infusions of LCK-GFP resulted in robust transduction of astrocytes in the hippocampal CA1 region. Staining for GluA1 (synaptic puncta) was also strong and consistent (**Figure 1A** and **B**). Neither AIE pre-exposure ($F_{(1,19.48)}$ = 0.27, P = 0.61) nor treatment in adulthood with gabapentin ($F_{(1,19.48)}$=0.05, P = 0.82) altered gross astrocyte morphology, expressed as the ratio of astrocyte surface area to astrocyte volume (**Figure 1C**). Further, there was no significant interaction of AIE with gabapentin with respect to that measure ($F_{(1,19.48)}$ = 2.52, P = 0.13).

Density of GluA1 synaptic puncta and protein expression

Similarly there was no effect of AIE ($F_{(1,24.73)}$=0.37, P = 0.52), gabapentin ($F_{(1,24.73)}$=3.17, P = 0.08), or their interaction ($F_{(1,24.73)}$=0.58, P = 0.46), on synaptic puncta density (**Figure 2A**). As an additional confirmation that AIE did not affect GluA1 expression we also measured the amount of GluA1 protein in area CA1 after AIE in a separate group of AIE and AIW animals. Here, adult GluA1 protein expression was not changed by AIE ($t_{(10)}$ = 0.72, P = 0.49; **Figure 2B**).

Astrocyte-synaptic proximity

In contrast to the lack of effect of AIE or gabapentin on CA1 astrocyte morphology, synaptic puncta density and GluA1 expression, AIE did alter the astrocyte-synapse interaction in area CA1. Simple main effects were used to test our specific hypotheses and revealed that, in cells from gabapentin naïve animals, AIE reduced colocalization of astrocyte plasma membrane with synaptic puncta when compared to AIW ($t_{(15.86)}$ = 1.89, P = 0.04; **Figure 1D**), indicating that AIE re-

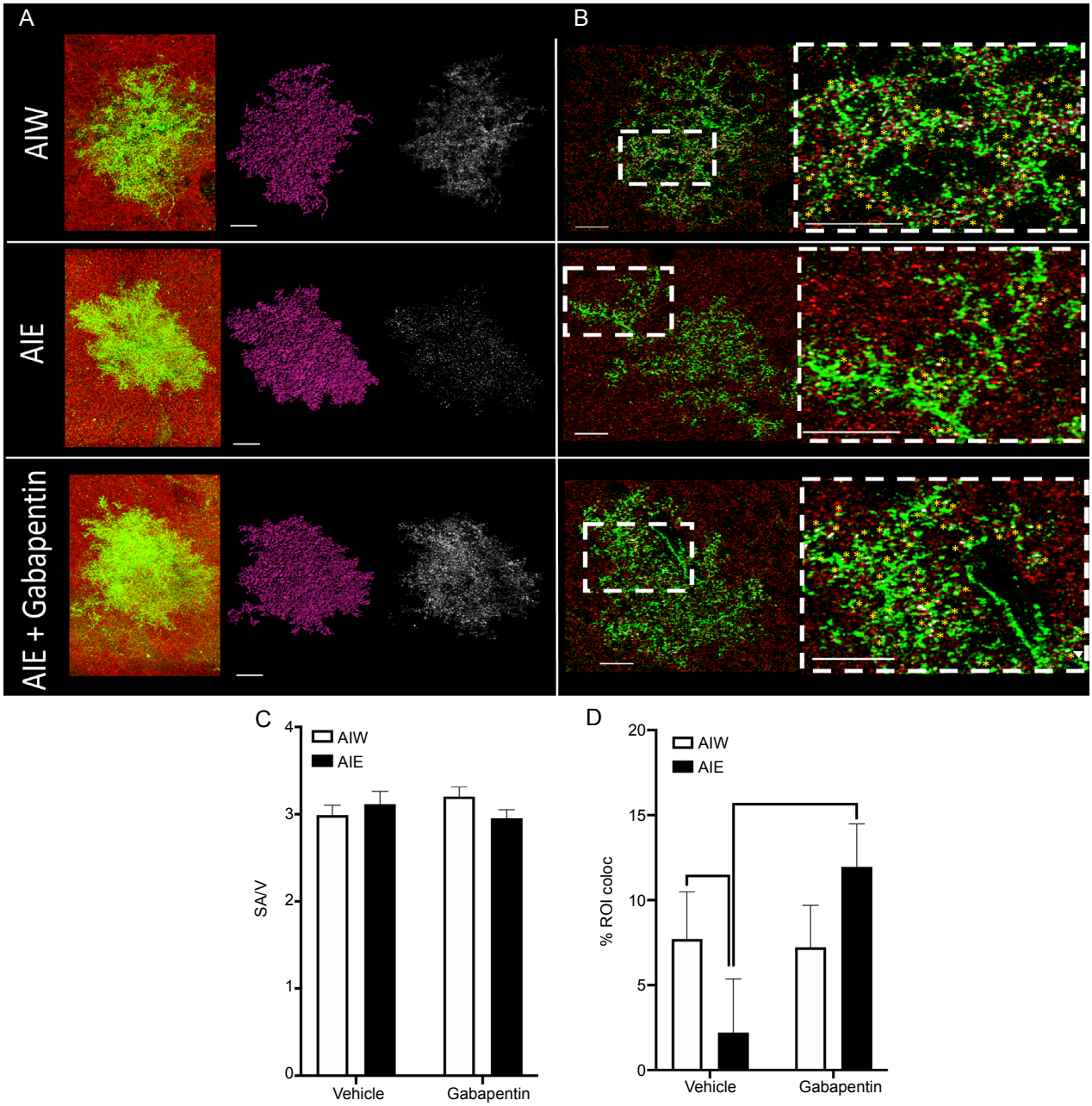

Figure 1 AIE-induced reduction of astrocyte-synapse proximity in hippocampal area CA1 is reversed by gabapentin.
(A) Left to right: Raw z-series astrocytes (green) and synaptic puncta (red), rendered astrocytes (purple), and points of colocalization of the astrocyte and synaptic maker (white), from control animals that received AIW, those exposed to AIE, and AIE animals that received gabapentin in adulthood (AIE + gabapentin). Scale bars: 15 μm. (B) Left Column: Astrocytes (green) and synaptic puncta (red) from each of the treatment groups described under A. Inset boxes represent regions for expanded magnification. Scale bars: 15 μm. Right column: Expanded magnification of areas inset in left column. Yellow asterisks indicate identified points of astrocyte-synaptic colocalization. Scale bars: 15 μm. (C) Mean (± SEM) ratio of astrocyte surface area (SA) to volume (V) was unchanged by AIE or Gabapentin treatment. (D) Mean (± SEM) percent of colocalization of astrocyte viral labeling and synaptic puncta was reduced in hippocampal area CA1 in adulthood following AIE ($P < 0.05$, *vs.* AIW), and this decrease was reversed by treatment with gabapentin ($P < 0.05$, *vs.* AIE and $P > 0.05$, *vs.* AIW + gabapentin). The number of animals used for each treatment group was: AIW – $n = 6$, AIE – $n = 6$, AIW + gabapentin – $n = 8$, AIE + gabapentin – $n = 7$. An average of five cells per animal were included in the mixed linear modeling analysis. AIE: Adolescent intermittent ethanol; AIW: adolescent intermittent water.

duced astrocyte synapse proximity. In addition, we observed increased colocalization in AIE animals that were treated with gabapentin, compared to those AIE treated animals that did not receive gabapentin ($t_{(16.53)} = –2.12$, $P = 0.03$), consistent with our hypothesis that gabapentin would reverse the effect of AIE on astrocyte-synapse interaction. There was no significant difference in synaptic proximity between astrocytes from AIE and AIW exposed animals that had received gabapentin ($t_{(16.16)} = –1.07$, $P = 0.15$), which provides further evidence that gabapentin treatment reversed the AIE-induced deficit on astrocyte-synapse interaction. To better understand the specificity of the gabapentin effect, %ROI colocalization was compared in cells from AIW animals that did not receive gabapentin to cells from AIW animals that did receive gabapentin. There was no significant effect of gabapentin on cells from AIW animals ($t_{(14.48)} = 0.26$, $P = 0.4$),

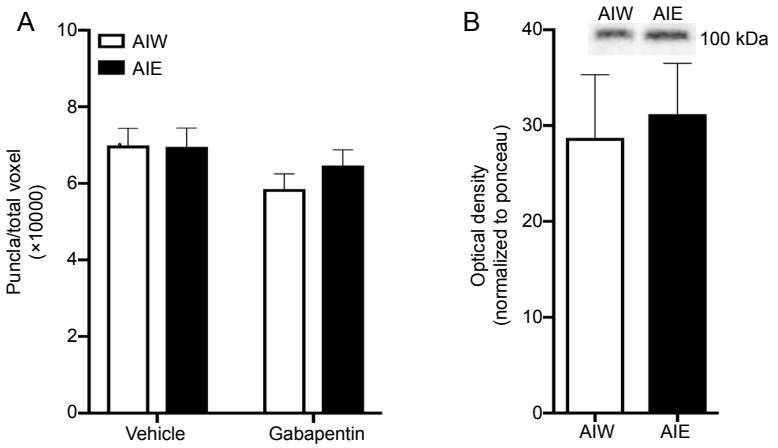

Figure 2 AIE does not affect the density of synaptic puncta, or GluA1 protein expression, in hippocampal area CA1 in adulthood.
(A) Mean (± SEM) punctate GluA1 signal detection performed using the Imaris spots function. There were no significant differences in the density of puncta across treatment groups. The number of puncta was normalized to total voxels of the z-stack dataset. (B) Mean (± SEM) normalized optical density from Western blot assessment of GluA1 protein expression. AIE did not affect GluA1 protein expression. Representative expression bands above. AIE: Adolescent intermittent ethanol; AIW: adolescent intermittent water; GluA1: AMPA receptor subunit GluR1.

indicating that the gabapentin effect was only present in cells from AIE animals. A significant interaction between AIE and gabapentin on % ROI colocalization between GFP and GluA1 was also present ($F_{(1,32.52)} = 3.43$, $P = 0.07$).

Discussion

The principal findings of this study are that in adulthood, following adolescent intermittent ethanol exposure, the extent of astrocytic synaptic contact, as measured with our colocalization assay, is diminished in hippocampal area CA1. Importantly, the effect of AIE on astrocyte-synapse proximity was reversed by sub-chronic treatment with gabapentin during adulthood. The persistence of the AIE effect into adulthood is notable as it indicates an enduring, regulatory change in astrocytic synaptic ensheathment, without an effect on overall astrocyte morphology or synaptic density. This is consistent with other enduring neural and behavioral effects of AIE (Crews et al., 2019). The present finding of AIE-induced reduction of astrocyte-synapse colocalization suggests the possibility that previously observed AIE-induced TSP and GFAP increases in adulthood (Risher et al., 2015a) could represent a compensatory upregulation to enhance synaptogenesis against the backdrop of reduced astrocytic synaptic insulation in local hippocampal circuits. Indeed, we have observed increases in excitatory signaling (Swartzwelder et al., 2017) and synaptic plasticity (Risher et al., 2015b) in area CA1 after AIE that could be the result of such a compensatory mechanism. Compounding this effect, a reduction in astrocytic synaptic coupling in the CA1 region would potentially impair glutamate clearance from the synapse, increasing neuronal excitability (Murphy-Royal et al., 2017). It is also notable that the observed AIE-induced reduction of astrocyte synapse proximity occurred in the absence of an effect on astrocyte morphology, suggesting that the effect of AIE was not related to changes in overall astrocyte structure. This distinction is consistent with previous studies demonstrating reductions in astrocyte neuronal proximity after methamphetamine exposure, in the absence of an overall effect on astrocyte morphology (Siemsen et al., 2019b). The fact that there was no effect of AIE on GluA1 puncta density is consistent with other recent studies (Contreras et al., 2019) and indicates that the principal effect of AIE was on astrocytes rather than on GluA1 expression on neurons. Interestingly, other studies from our laboratory indicate in increase in NMDA (specifically GluN2B) receptor activity in the hippocampal formation in adulthood after AIE (Swartzwelder et al., 2017), suggesting a greater propensity toward synaptic plasticity after AIE in the absence of significant change in ongoing baseline excitatory function. Such changes could be related to the effects of AIE on dendritic spine development and morphology after AIE (Risher et al., 2015a, b; Mulholland et al., 2018). It is notable, however, that only one dose of ethanol was used for both ethanol exposure and gabapentin treatment. Thus, these finding do not address the potency of these drugs. In addition, the present data do not address the duration of the gabapentin reversal of AIE effects as we assessed only one time point after gabapentin treatment. Therefore, an assessment of the reversal duration must await future research.

Indeed, it would be expected that astrocyte-neuron synaptic decoupling would cause a shift in dendritic spine types, and thereby alter synaptic function. We have previously reported that AIE results in a greater proportion of elongated, long-thin spines on neurons in hippocampal area CA1 (Mulholland et al., 2018). Potential new targets include astrocyte released ephrin A3, which targets EphA4 receptors and influences spine shape. Ephrin A3 is highly localized in the regions of astrocyte membranes that are colocalized with neuronal synaptic regions and activates neuronal EphA4 receptors (Carmona et al., 2009). This results in an induced decrease in hippocampal dendritic spine length, characteristic of stable synapses and less plastic spine function (Carmona et al., 2009). Decreases of EphA4, which can be caused by a reduction of astrocyte-released ephrin A3, result in elongation and disorganization of spine morphology, similar to our previous observations (Risher et al., 2015b; Mulholland et al., 2018). Thus, the present findings suggest that effect could be due to reduced astrocyte-synapse coupling, resulting in a degrading of the usual ephrin A3-EphA4 interaction, and elucidating an interesting new area of study.

Our findings describing a reversal of AIE-induced astrocyte retraction from synapses following adult treatment with gabapentin is notable because of its translational significance. Gabapentin is a widely used clinical agent for the treatment of neurological and psychiatric disorders (Montastruc et al., 2018). Thus, its safety and efficacy profile are well known. Although gabapentin's possible usefulness as a treatment for enduring neurobehavioral sequelae of adolescent alcohol use in humans remains to be determined, its efficacy in this animal model suggests that possibility. Additionally, these

findings also point in the direction of potential mechanisms underlying AIE effects on hippocampal circuitry and function. This observed reversal of hippocampal AIE effects is consistent with a previous report in which exposure of hippocampal slices to gabapentin *in vitro* reversed the effects of AIE on NMDA receptor-mediated synaptic currents in CA1 pyramidal cells (Swartzwelder et al., 2017). If AIE-induced de-coupling of astrocytes and neurons (as demonstrated in the present data) results in a compensatory TSP-induced increase in excitatory synaptogenesis that leads to increased NMDA current amplitude (Swartzwelder et al., 2017), then gabapentin might decrease that amplitude increase by antagonizing the excitatory synaptogenic effect of TSPs at their neuronal a2 1 receptor (Eroglu, 2009).

In summary, the present findings identify, for the first time, an effect of adolescent alcohol exposure on astrocyte-neuronal synaptic proximity that endures into adulthood and the reversal of that effect by a pharmaceutical agent in common use. Thus, their translational significance is obvious. In addition, these findings suggest specific mechanisms, related to the impact of astrocyte-neuronal interactions on dendritic spine morphology that might underlie previously reported effects of AIE on synaptic and behavioral functions.

Author contributions: *Viral infusions, imaging and immunohistochemistry, experimental design, and document preparation: KLH. Animal treatments, viral infusions, data management, and document preparation: SK. Animal treatments and viral infusions: SH. Virus preparation, experimental design, and document preparation: KJR. Experimental design, initial immunohistochemistry and imaging: AT. Western blot studies: TAW. Statistical analyses: SKA. Imaging, cell identification and quantification: BMS and JAM. Experimental design, imaging, immunohistochemistry interpretation, document preparation: MDS. Project conceptualization, experimental design, statistical analyses, document initiation and preparation: HSS. All authors approved the final manuscript.*
Conflicts of interest: *None declared.*
Financial support: *This study was supported by the National Institute on Alcohol Abuse and Alcoholism (NIAAA) Neurobiology of Adolescent Drinking In Adulthood (NADIA) Grant # 2U01AA019925 (to HSS); the National Institute on Alcohol Abuse and Alcoholism (NIAAA) R00AA022651 (to TAW); the National Institute on Drug Abuse (NIDA) R01DA041455 (to KJR).*
Institutional review board statement: *The animal experiments were approved by the Duke University Institutional Animal Care and Use Committee (Protocol Registry Number A159-18-07) on July 27, 2018.*
Copyright license agreement: *The Copyright License Agreement has been signed by all authors before publication.*
Data sharing statement: *Datasets analyzed during the current study are available from the corresponding author on reasonable request.*
Plagiarism check: *Checked twice by iThenticate.*
Peer review: *Externally peer reviewed.*

Open peer reviewer: *Adriana Vizuete, Universidade Federal do Rio Grande do Sul Instituto de Ciencias Basicas da Saude Biochemistry, Brazil.*

References

Aarts E, Verhage M, Veenvliet JV, Dolan CV, van der Sluis S (2014) A solution to dependency: using multilevel analysis to accommodate nested data. Nat Neurosci 17:491-496.

Baucum AJ, 2nd, Brown AM, Colbran RJ (2013) Differential association of postsynaptic signaling protein complexes in striatum and hippocampus. J Neurochem 124:490-501.

Carmona MA, Murai KK, Wang L, Roberts AJ, Pasquale EB (2009) Glial ephrin-A3 regulates hippocampal dendritic spine morphology and glutamate transport. Proc Natl Acad Sci U S A 106:12524-12529.

Contreras A, Polin E, Miguens M, Perez-Garcia C, Perez V, Ruiz-Gayo M, Morales L, Del Olmo N (2019) Intermittent-excessive and chronic-moderate ethanol intake during adolescence impair spatial learning, memory and cognitive flexibility in the adulthood. Neuroscience 418:205-217.

Costes SV, Daelemans D, Cho EH, Dobbin Z, Pavlakis G, Lockett S (2004) Automatic and quantitative measurement of protein-protein colocalization in live cells. Biophys J 86:3993-4003.

Crews FT, Robinson DL, Chandler LJ, Ehlers CL, Mulholland PJ, Pandey SC, Rodd ZA, Spear LP, Swartzwelder HS, Vetreno RP (2019) Mechanisms of persistent neurobiological changes following adolescent alcohol exposure: NADIA consortium findings. Alcohol Clin Exp Res 43:1806-1822.

Dawson DA, Goldstein RB, Chou SP, Ruan WJ, Grant BF (2008) Age at first drink and the first incidence of adult-onset DSM-IV alcohol use disorders. Alcohol Clin Exp Res 32:2149-2160.

Eroglu C (2009) The role of astrocyte-secreted matricellular proteins in central nervous system development and function. J Cell Commun Signal 3:167-176.

Gustin RM, Shonesy BC, Robinson SL, Rentz TJ, Baucum AJ 2nd, Jalan-Sakrikar N, Winder DG, Stanwood GD, Colbran RJ (2011) Loss of Thr286 phosphorylation disrupts synaptic CaMKIIα targeting, NMDAR activity and behavior in pre-adolescent mice. Mol Cell Neurosci 47:286-292.

Lees B, Mewton L, Stapinski LA, Squeglia LM, Rae CD, Teesson M (2019) Neurobiological and cognitive profile of young binge drinkers: a systematic review and meta-analysis. Neuropsychol Rev 29:357-385.

Montastruc F, Loo SY, Renoux C (2018) Trends in first gabapentin and pregabalin prescriptions in primary care in the United Kingdom, 1993-2017. JAMA 320:2149-2151.

Mulholland PJ, Teppen TL, Miller KM, Sexton HG, Pandey SC, Swartzwelder HS (2018) Donepezil reverses dendritic spine morphology adaptations and Fmr1 epigenetic modifications in hippocampus of adult rats after adolescent alcohol exposure. Alcohol Clin Exp Res 42:706-717.

Murphy-Royal C, Dupuis J, Groc L, Oliet SHR (2017) Astroglial glutamate transporters in the brain: Regulating neurotransmitter homeostasis and synaptic transmission. J Neurosci Res 95:2140-2151.

Paxinos G, Watson C (1986) The rat brain in stereotaxic coordinates, 2nd ed. San Diego, CA: Academic Press.

Risher ML, Fleming RL, Boutros N, Semenova S, Wilson WA, Levin ED, Markou A, Swartzwelder HS, Acheson SK (2013) Long-term effects of chronic intermittent ethanol exposure in adolescent and adult rats: radial-arm maze performance and operant food reinforced responding. PLoS One 8:e62940.

Risher ML, Sexton HG, Risher WC, Wilson WA, Fleming RL, Madison RD, Moore SD, Eroglu C, Swartzwelder HS (2015a) Adolescent intermittent alcohol exposure: dysregulation of thrombospondins and synapse formation are associated with decreased neuronal density in the adult hippocampus. Alcohol Clin Exp Res 39:2403-2413.

Risher ML, Fleming RL, Risher WC, Miller KM, Klein RC, Wills T, Acheson SK, Moore SD, Wilson WA, Eroglu C, Swartzwelder HS (2015b) Adolescent intermittent alcohol exposure: persistence of structural and functional hippocampal abnormalities into adulthood. Alcohol Clin Exp Res 39:989-997.

Scofield MD, Li H, Siemsen BM, Healey KL, Tran PK, Woronoff N, Boger HA, Kalivas PW, Reissner KJ (2016) Cocaine self-administration and extinction leads to reduced glial fibrillary acidic protein expression and morphometric features of astrocytes in the nucleus accumbens core. Biol Psychiatry 80:207-215.

Siemsen BM, Giannotti G, McFaddin JA, Scofield MD, McGinty JF (2019a) Biphasic effect of abstinence duration following cocaine self-administration on spine morphology and plasticity-related proteins in prelimbic cortical neurons projecting to the nucleus accumbens core. Brain Struct Funct 224:741-758.

Siemsen BM, Reichel CM, Leong KC, Garcia-Keller C, Gipson CD, Spencer S, McFaddin JA, Hooker KN, Kalivas PW, Scofield MD (2019b) Effects of methamphetamine self-administration and extinction on astrocyte structure and function in the nucleus accumbens core. Neuroscience 406:528-541.

Snedecor GW, Cochran WG (1989) Statistical methods, 8th ed. Ames, Iowa: Iowa State University Press.

Spear LP (2018) Effects of adolescent alcohol consumption on the brain and behaviour. Nat Rev Neurosci 19:197-214.

Swartzwelder HS, Park MH, Acheson S (2017) Adolescent ethanol exposure enhances NMDA receptor-mediated currents in hippocampal neurons: reversal by gabapentin. Sci Rep 7:13133.

Swartzwelder HS, Healey KL, Liu W, Dubester K, Miller KM, Crews FT (2019) Changes in neuroimmune and neuronal death markers after adolescent alcohol exposure in rats are reversed by donepezil. Sci Rep 9:12110.

Testen A, Sepulveda-Orengo MT, Gaines CH, Reissner KJ (2018) Region-specific reductions in morphometric properties and synaptic colocalization of astrocytes following cocaine self-administration and extinction. Front Cell Neurosci 12:246.

Testen A, Ali M, Sexton HG, Hodges S, Dubester K, Reissner KJ, Swartzwelder HS, Risher ML (2019) Region-specific differences in morphometric features and synaptic colocalization of astrocytes during development. Neuroscience 400:98-109.

Volterra A, Meldolesi J (2005) Astrocytes, from brain glue to communication elements: the revolution continues. Nat Rev Neurosci 6:626-640.

P-Reviewer: Vizuete A; C-Editors: Zhao M, Li CH; T-Editor: Jia Y